Water Research 201 (2021) 117332

Contents lists available at ScienceDirect

Water Research

journal homepage: www.elsevier.com/locate/watres

Interplay of oxygen and light in the photo-oxidation of dissolved organic carbon

Ora E. Johannsson [a,*], Marcio S. Ferreira [b], D. Scott Smith [c], Chris M. Wood [a,b], Adalberto L. Val [b]

[a] Zoology Department, University of British Columbia, Vancouver, BC, V6T 1Z4 Canada
[b] Laboratory of Ecophysiology and Molecular Evolution, Brazilian National Institute for Research of the Amazon, INPA, Manaus, AM, Brazil
[c] Department of Chemistry and Biochemistry, Wilfrid Laurier University, Waterloo, ON, N2L 3C5 Canada

ARTICLE INFO

Keywords:
Areal photo-oxidation
Fluorescence
Absorbance
Amazon
Rio Negro

ABSTRACT

Light energy and oxygen drive photo-oxidation of dissolved organic carbon (DOC). The longer the wavelength the greater its depth of penetration into water, changing the spectral environment with depth. We asked how oxygen concentration and light spectral composition might affect photo-oxidation processes in DOC. Outdoor experiments compared responses of fluorescence and absorbance indices to photo-oxidation of filtered (0.45 μm) Rio Negro water (Amazon Basin) under near-anoxia, normoxia and hyperoxia exposed to natural sunlight or reduced sunlight (≥340, reduced-UVR). Near-anoxia decreased all absorbance and fluorescence indices. Absorbance changed across the spectrum (≥250 nm) even under reduced-UVR provided that oxygen was present. This phenomenon maintains broader photo-oxidation and the release of CO_2 at depth. $Slope_{350–400}$ was responsive to changes in the irradiance field but not to oxygen concentration, while $Slope_{275–295}$ responded to both. Thus, larger molecules are broken down near the water's surface and medium to smaller molecules continue to be processed at depth. The production of fulvic acid-like fluorescence required both UVB and oxygen, restricting its production to surface waters. The relatively small increase in $R_{254/365}$ compared with the loss of $SUVA_{254}$ under near-anoxia indicated a slower breakdown of larger DOC molecules as oxygen becomes limiting. Breakdown of larger molecules which absorb in the 350–400 nm range, appears to involve two steps – one by radiant energy and another involving oxygen. The study results reflect the dynamic gradients in photo-oxidation with depth.

1. Introduction

Photo-oxidation is the breakdown of molecular compounds by the energy contained in light. Both ultraviolet radiation [UVR: UVA, 320–400 nm, and UVB, 280–320 nm wavelengths] and photosynthetically active radiation [PAR, 400–700 nm wavelengths] contribute to the photo-oxidation of dissolved organic carbon (DOC). Each wavelength carries a specific level of energy which is an inverse function of wavelength - the shorter the wavelength, the higher the energy content. In terms of CO_2 production in natural waters, UVA and PAR are equally important (37% - 44%) while UBV is less important (15% - 17%) (Granéli et al., 1998; Zhang and Xie, 2015). The proportionate contribution will vary with DOC composition. For instance, Wang et al. (2009) using Suwannee River humic acid alone found a ratio of 31.8%: 32.6% to 25.6% for UBV:UVA:PAR. These data indicate that UVB may be particularly important in breaking down the larger humic molecules.

The contribution of UVR and PAR to photo-oxidation will change with depth. The depth of penetration of radiant (light) energy into water is a function of radiation intensity and wavelength: the longer the wavelength, the greater the depth of potential penetration (Kirk 1994). Penetration is attenuated by the processes of absorbance and scattering in an approximately exponentially manner (Kirk, 1994). Absorbance reduces the intensity of radiation. Plankton, dissolved organic and inorganic matter, and water absorb UVR and PAR (Kirk, 1994). Scattering decreases the downward intensity by redirecting light above and lateral to the line of descent. Scattering is a function of colloidal and particle density, size and shape (Kirk 1994). Due to the nature of light and these processes, gradients in photon concentration and radiant energy are established in the water column. Higher photon concentrations, particularly of the more energetic UVB, occur near the surface. Lower

* Corresponding author.
E-mail addresses: johannss@zoology.ubc.ca (O.E. Johannsson), marcio@inpa.gov.br (M.S. Ferreira), ssmith@wlu.ca (D.S. Smith), woodcm@zoology.ubc.ca (C.M. Wood).

https://doi.org/10.1016/j.watres.2021.117332
Received 3 February 2021; Received in revised form 14 May 2021; Accepted 1 June 2021
Available online 8 June 2021

photon concentrations, mainly of the lower energy PAR, occur at depth. We know that the rate of complete photo-oxidation (production of CO_2) decreases with depth (e.g. Granéli et al., 1996; Johannsson et al., 2020). We might expect that the greater loss of UVR with depth also affects the processes of photo-oxidation of DOC.

Photo-oxidation of DOC usually involves the incorporation of oxygen (Lindell and Rai, 1994; Amon and Brenner, 1996; Patel-Sorrentino et al., 2004; Xie et al., 2004; Cory et al., 2014). Unsaturated carbon bonds of aromatic compounds are broken by radiant energy, either directly or through the production and activity of reactive oxygen species (ROS) and excited electrons, with the incorporation of oxygen and hydrogen (Vähätalo et al., 1999; Gonsior et al., 2009; Cory et al., 2010; Ward and Cory, 2016; McKay 2020). Most of the incorporated oxygen comes directly from the environment (Cory et al., 2010). Oxygen is one of a number of variables that influences the rates of photo-oxidation and how DOC is degraded (Gao and Zepp, 1998; Lou et al., 2006; Helms et al., 2008; Gonsior et al., 2009; Zhang and Xie, 2015). The total amount of oxygen consumed by photo-oxidation is not negligible, but approximates the amount released as CO_2 (e.g. Amon and Benner 1996; Xie et al., 2004).

The present study extends this work by examining the relationship between oxygen concentration and structural degradation of DOC with particular emphasis on how this relationship changes with changes in the radiation field with depth.

The question is not trivial. Low oxygen concentrations in surface waters are common in freshwater and nearshore environments (Wu, 2002; Smith et al., 2006; Diaz and Breitburg, 2009). They can occur both naturally and due to anthropogenic activities (e.g., Daniel et al., 2002). In the Amazon Basin, where this study was undertaken, oxygen concentrations are typically greater than 3 mg $O_2.l^{-1}$ (Richey et al., 1990; Rasera et al., 2013; Johannsson et al., 2017). However, oxygen levels between 0.8 and 2.6 mg $O_2.l^{-1}$ have been observed in surface waters during the day at various times during the year (Amaral et al., 2019, Supplementary Table S1). In the Jutaí and Purus Rivers, minimum values of 1.9 and 1.3 mg $O_2.l^{-1}$ were observed during falling waters, in the Jutaí, Juruá and Purus Rivers, minimum values ranged from 1.9 to 2.4 mg $O_2.l^{-1}$ during rising waters (Richey et al., 1990). In the Rio Negro, near Barcelos, oxygen levels of 1.5 to 2.6 mg $O_2.l^{-1}$ were recorded during the day and night, from 2 m depth to the surface in April 2012 (unpublished data, Z. Gallagher, O. E Johannsson, and A.L. Val). Oxygen extremes ($\sim$19mg$O_2.l^{-1}$) can occur in some small near-river lakes during falling water (Val-and Almeida-Val, 1995).

Photo-oxidation of DOC comprises numerous chemical reactions involving the breakdown of molecules with the incorporation of oxygen and increase in unsaturated bonds until eventually CO_2 and CO are produced. We hypothesize that these various chemical reactions will be differentially affected by oxygen concentration and radiant energy species (UVB, UVA, PAR), and that these variables, of oxygen and radiation, may interact, likely through the movement of excited electrons and ROS. Given these thoughts and the opportunity for photo-oxidation of DOC to occur under conditions ranging from hypoxic/anoxic to hyperoxic, and under complete (surface) and reduced (at depth) radiation fields, the objective of the present study was to determine the relationships between oxygen concentration, radiation field and photo-oxidation. We monitored the changes in DOC structure under full-spectrum, natural light and under reduced-UVR exposure (no UVB) at three oxygen exposures, near-anoxia, normoxia and hyperoxia, using absorbance and fluorescence spectrophotometry.

2. Methods

Experiments with Rio Negro water were conducted outdoors at the Instituto Nacional de Pesquisas da Amazônia (INPA) in Brazil in December 2015 and October 2018. Experimental water was collected from the center of the river channel, upstream of Manaus - 56 km above the confluence of the Solimões and Rio Negro rivers, which form the Amazon River – the same location used by Johannsson et al., (2020). Water was filtered through 0.45 μm polyethersulfone or cellulose acetate filters, and stored at <4 °C. The experimental protocols of Johannsson et al., (2020) were followed and are briefly described in Supplementary Materials. Only information specific to this study is presented here. Conditions during each experiment are found in Table 1.

2.1. Light

Complete and partial light exposures were obtained by using two different experimental vessels – quartz tubes and flint bottles. Transmission of UVR and PAR through 1.5 mm thick quartz glass is >92%, (Techinical Glass Products, 2020, http://www.technicalglass.com/fused_quartz_transmission.html). UVR transmission through flint quartz was reduced, increasing from 0% at 300 nm to 82% for wavelengths ≥350 nm (Fig. 12 in Dias et al., 2010). The quartz tubes were 1.8 cm in diameter with a volume of 35 ml; the flint bottles were 5 cm in diameter with a volume of 120 ml. UVR reaching the center of the quartz tubes was ~56% of subsurface radiation while that of the flint bottles was ~31%. The estimates were based on Beer-Lambert absorbance decay of sample initial absorbance values and assumed equal quantities of photons at all wavelengths

2.2. Oxygen treatments

Filtered water was warmed to experimental temperature (30 °C). Oxygen content was adjusted by bubbling with nitrogen, air or oxygen. Oxygen concentration was measured using a Microx TX3 [Presens Precision Sensing GmbH (Regensburg, Germany, www.presens.de), 2018] or a YSI 55 dissolved oxygen probe [YSI (Xylem, Rye Brook, NY, USA), 2015]. Water was siphoned into each quartz tube or bottle until overflowing in order to maintain the oxygen concentration. Three oxygen treatments were run: near-anoxia (0.3 mg$O_2.l^{-1}$and 0.2 mg$O_2.l^{-1}$), normoxia (8.4 mg$O_2.l^{-1}$ and 7.1 mg $O_2.l^{-1}$) and hyperoxia (19.3 mgO_2. l^{-1} and 17.4 mg$O_2.l^{-1}$) (Table 1). All tubes/bottles were checked to ensure no bubbles were present. The dark tubes/bottles were wrapped in aluminum foil.

2.3. Sample analyses

Total DOC was measured on a high-temperature Shimadzu TOC-V_{CSH} Total Organic Carbon (TOC) Analyzer (Shimadzu, Kyoto 604–8511, Japan). Manufacturer recommended standards and ultrapure water blanks were run at the same time.

In 2015, absorbance profiles were collected from 250 to 550 nm at 10-nm intervals on a SpectraMax Plus 384 spectrophotometer (Molecular Devices, Sunnyvale, CA 94,089, USA) using a 1-cm, pathlength, quartz cuvette. Fluorescence emission profiles were measured from 250 to 550 nm at 10-nm intervals using four excitation wavelengths (250, 300, 325, and 370 nm) using the SpectraMax Plus 384 spectrophotometer and fluorescence software. In 2018, fluorescence and absorbance data were measured similarly using a Horiba Aqualog (Horiba Ltd., Kyoto, Japan). Ultrapure water blanks were run each day for all spectrophotometric work.

Spectrophotometric indices were used to follow changes in DOC composition (Table 2). Two measures track the decrease in aromatic hydrocarbons. $SUVA_{254}$, the absorbance at 254 nm normalized to DOC, is correlated with total aromaticity and molecular weight (Abbt-Braun et al., 2004; Chowdhury, 2013). SAC_{340}, the absorbance coefficient at 340 nm normalized to DOC, correlates with DOC aromaticity, and DOC's protective capacity in fish against low pH and certain metal toxicities (Wood et al., 2011; Al Reasi et al., 2013). The ratio ($R_{254/365}$) is correlated with E2E3, the ratio $R_{250/365}$ (Suppl. Fig. S1): both track mean molecular size (Dahlén et al., 1996; Lou and Xie, 2006). SAC_{Ka310} is a measure of the capacity of DOC to produce ROS (Scully et al., 1996; Johannsson et al., 2017).

Table 1
Dates and environmental conditions of experiments conducted at INPA, Manaus, Brazil. We examined the effect of oxygen concentration and spectrum of UVR exposure on absorbance and fluorescence losses on photo-oxidation of Rio Negro DOC. The experiments were run in either flint bottles (reduced-UVR) or quartz tubes (complete-UVR). UVR and temperature were monitored at 30-minute intervals. See Methods 2.0–2.3 and Supplementary Materials for experimental details.

Date	Container	Oxygen Range ($mgO_2.l^{-1}$)	Temperature (°C)	Total UV Radiation ($mW.cm^{-2}$)	Hours of Light (h)
Dec. 2015	Flint bottles	0.3 – 19.4	29.7	122.7	30.8
Oct. 2018	Quartz tubes	0.2 – 17.4	32.8	128.2	18.8

Table 2
Absorbance and fluorescence indices used in the present study, their calculation, relevance and source. This table is a modification of the one presented in Johannsson et al., (2020).

	Name (units)	Calculation	Relevance	References
Absorbance Indices	SAC_{340} ($cm^2.mgC^{-1}$)	Specific absorbance at 340 nm: absorbance at 340 nm * 2.303. DOC^{-1} *1000)	Measure of aromaticity, protective potential of the DOC against some metals, and potential for direct biological effects on organisms	Curtis and Schindler (1997) Wood et al., (2011) Al-Reasi et al., (2012) Al-Reasi et al., (2013)
	SAC_{Ka310} ($cm^2.mgC^{-1}$)	Specific absorbance at 310 nm: 2.303 * absorption at 310 nm/path length (0.01 m).DOC^{-1}	Measure of potential production of oxygen radicals per unit of DOC	Scully et al., (1996) Johannsson et al., (2017)
	$R_{254/365}$	Ratio of absorbance at 254 nm to that at 365 nm	Index of the average molecular mass within the DOC	Dahlén et al., (1996)
	$SUVA_{254}$ ($cm^2.mgC^{-1}$)	Absorbance at 254 nm/ pathlength (0.01 m).DOC^{-1}	Measure of aromaticity, molecular weight, hydrophobic organic acid fraction	Abbt-Braun et al., (2004) Weishaar et al., (2003) Spencer et al., (2012) Chowdhury (2013) Hansen et al., (2016)
	$Slope_{275–295}$ ($cm^{-1}.nm^{-1}$)	Slope of regression of the ln of absorbances from 275 to 295 nm	Index of molecular weight – correlated with weight of fulvic acid like compounds (but not humic acid-like compounds). Tracer of changes in DOC structure	Helms et al., (2008) Hayase and Tsubota (1985) Carder et al., (1989)
	$Slope_{350–400}$ ($cm^{-1}.nm^{-1}$)	Slope of regression of the ln of absorbances from 350 to 400 nm	Reflects changes in high molecular weight compounds	Helms et al., (2008)

Degradation of larger molecules into smaller molecules is captured in the slope indices. Absorbance data, plotted against wavelength, decline in a roughly exponential function. The natural log of the absorbance data is basically straight over narrow ranges. The slope of the linear regression of the ln data, calculated over the wavelength range 275 – 295 nm ($Slope_{275–295}$), correlates with mean molecular weight. Changes in this slope, and $Slope_{350–400}$, reflect shifts in the proportion of smaller to larger molecules in these portions of the curve (Helms et al., 2008). During photo-oxidation, $Slope_{275–295}$ becomes steeper and $Slope_{350–400}$ flattens (Helms et al., 2008).

Two fluorescence metrics captured major portions of the humic acid-like (HA) and fulvic acid-like (FA) moieties (Table 3) consistently in Rio Negro waters (Johannsson et al., 2020). The metrics sum the emission profiles across specific segments of each of the four excitation wavelengths measured (Table 3). These summed metrics can be compared across treatments in order to characterize changes in the DOC composition and structure. The loss of fluorescence can be due to either destruction of the fluorophore and/or change in its redox state. Photo-oxidation pushes fluorophores towards a more oxidized state which has a diminished fluorescence, and shifts the location of the maximum emission toward smaller wavelengths (Cory and McKnight, 2005). Therefore, changes in location of the maximum emission were noted.

2.4. Data analysis

For all indices, the light-exposed values were subtracted from the average dark value for each treatment to determine the change due to photo-oxidation (Δvalues). Each treatment had equal numbers of light and dark replicates. Thus, positive Δvalues are a loss or decrease in the index, and negative Δvalues are a gain or increase in the index.

The use of parametric or non-parametric tests was determined by normality (Shapiro-Wilk Normality Test) and equality of variance (Bartlet's Test) tests. Parametric tests included one-way Analysis of Variance followed by Tukey's Multiple Comparisons Test, or a Student's t-Test if only two treatments were compared. Non-parametric tests included the Kruskal-Wallis one-way Analysis of Variance followed by Dunn's Multiple Comparison Test, or the Mann-Whitney U Test when two treatments were compared. The significance level of 0.05 was accepted. Means are reported ± 1 SEM (n), unless otherwise noted. All analyses were carried out in Graphpad PRISM 7 or 8 (Graphpad Software Inc, CA, USA (www.graphpad.com/scientific-software/prism)).

3. Results

Significant changes in absorbance were observed at all wavelengths and treatments with the exception of reduced-UVR/near-anoxia. In that treatment, dark control and light exposed absorbances were not

Table 3
The excitation wavelengths of the fluorescence metrics and their corresponding portions of the emission profile. The metrics capture a large portion of the fluorescence response of humic acid-like (HA), and fulvic acid-like (FA) compounds. The emission ranges are based on PARAFAC analyses of Rio Negro water (modified from Johannsson et al., (2020)).

Excitation Wavelength (nm)	Emission ResponseRange (nm)	Composition
370	400 - 550	HA
325	400 - 450	FA
	460 - 550	HA
300	400 - 450	FA
	460 - 550	HA
250	400 - 450	FA
	460 - 550	HA

statistically different at wavelengths <290 nm and >340 nm, based on one-tailed t-tests.

3.1. Absorbance indices

Oxygen limitation of photo-oxidative breakdown of DOC was evident under near-anoxia in all absorbance indices ($SUVA_{254}$, SAC_{340}, SAC_{Ka310}, and $R_{254/365}$) (Fig. 1A-D, Fig. 2A-D). $SUVA_{254}$, SAC_{340} and SAC_{Ka310} decreased by 30% to 40% under complete-UVR. $R_{254/365}$ was the exception, decreasing by 65%. Only SAC_{340} and SAC_{Ka310} showed significant decreases in absorbance under reduced-UVR (Table 4). These losses were ~55% lower than those under complete-UVR. Absorbance losses were not significantly different between normoxic and hyperoxic treatments (Figs. 1A-D, 2A-D).

To better visualize the impacts of lower oxygen concentrations across the absorbance spectrum, mean light absorbance was subtracted from mean dark absorbance for each measured wavelength from 250 to 400 nm for both the complete- and reduced-UVR treatments (Fig. 3A, B). The percentage loss of absorbance under normoxia and near-anoxia (Δabsorbance/dark controls*100%) was calculated (Fig. 3C). The ratio of Δnear-anoxia/Δnormoxia was calculated for each wavelength from the data of Figs. 3A and B, and a composite graph was created of these data (Fig. 4). Under complete-UVR, the pattern of loss of absorbance across wavelengths under normoxia and near-anoxia were similar but quantitatively different (Fig. 3A, curves N, and N-A). Three distinct regions were observed in the profile: 250 – 270 nm, 270 – 300 nm, and 300 – 400 nm (Fig. 3A). Profiles of the percentage loss in absorbance did not follow the same patterns as the profiles of absorbance loss against wavelength. Instead, the curves increased to a maximum near 300 nm and then declined (Fig. 3C).

Reduced-UVR responses showed much greater dependence on the presence of oxygen than the responses under complete-UVR, as seen by the difference between the normoxic and near-anoxic responses in each UVR treatment (Figs. 3A and B). Under reduced-UVR, the pattern of absorbance loss under normoxia extended to the lower wavelengths, thus making it appear similar to absorbance losses under complete-UVR (Figs. 3A and B, curves N). Closer inspection revealed a hollowing out of the curve between 250 – 300 nm. The pattern of absorbance loss under near-anoxia/reduced-UVR was not extended to lower wavelengths, but was greatly collapsed, especially at the shortest wavelengths, 250 to 280 nm (Fig. 3B, curve N-A). Curve N-A (Fig. 3B), then increased to a shallow peak between 300 - 320 nm – also seen in the normoxic curve. Absorbance losses in hyperoxia were greater than in normoxia under reduced-UVR, but less than those in normoxia in complete-UVR (Figs. 3A and B).

The absorbance ratios provided a clearer picture of the role of oxygen and UVR. The flat, upper line labelled 'a' in Fig. 4 at 1.0, is hypothetical, and represents a line of no impact of near-anoxia on absorbance loss. Curve 'b' is the ratio of Δnear-anoxia/Δnormoxia for DOC exposed to complete-UVR and curve 'c' is the ratio of Δnear-anoxia/Δnormoxia for DOC exposed to reduced-UVR (wavelengths >350 nm). The top area 'A' is the proportionate loss in photo-oxidation due to lack of oxygen across wavelengths from 250 to 400 nm. The area '*B* + C' is the proportion of photo-oxidation that remains under complete-UVR and lack of oxygen, and 'C' is the proportion of photo-oxidation that remains across wavelengths under reduced-UVR and lack of oxygen. The Δnear-anoxia/Δnormoxia ratios under complete-UVR were similar along the absorbance spectrum from 250 to 360 nm with a slight decline as of 300 nm and a steeper decline above 360 nm. Under reduced-UVR, the ratios were low (0.10 – 0.15) from 250 to 280 nm, because no significant change in absorbance occurred in the near-anoxia treatment. A peak in the ratio occurred between 300 and 340 nm, followed by a steep decline.

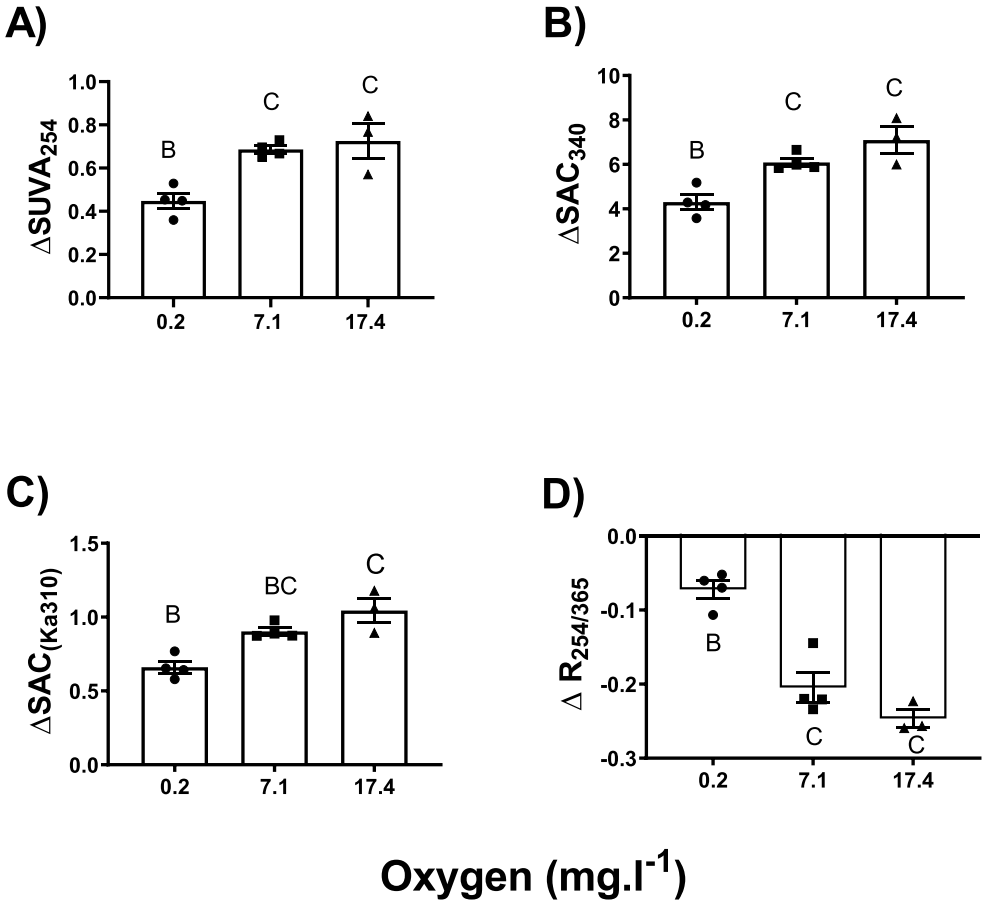

Fig. 1. Changes (Δ) in absorbance indices during photo-oxidation at three oxygen concentrations (near-anoxia, normoxia, hyperoxia) under complete-UVR exposure. (A) $\Delta SUVA_{254}$, (B) ΔSAC_{340}, (C) ΔSAC_{Ka310}, and (D) $\Delta R_{254/365}$. See Methods Section 2.4 and Table 2 for the meaning of the absorbance indices. Positive numbers indicate a loss of absorbance after photo-oxidation, while negative numbers indicate an increase in absorbance. See Table 1 for experimental conditions. Kruskal-Wallis ANOVA was employed for SAC_{Ka310} followed by Dunn's multiple comparisons tests (Kruskal-Wallis$_{(3,11)}$ = 8.326, p = 0.0012). For all other indices, ANOVA F-values were > 7 and p-values <0.0138. n = 4, 4, 3. Different letters above the bars indicate significant differences.

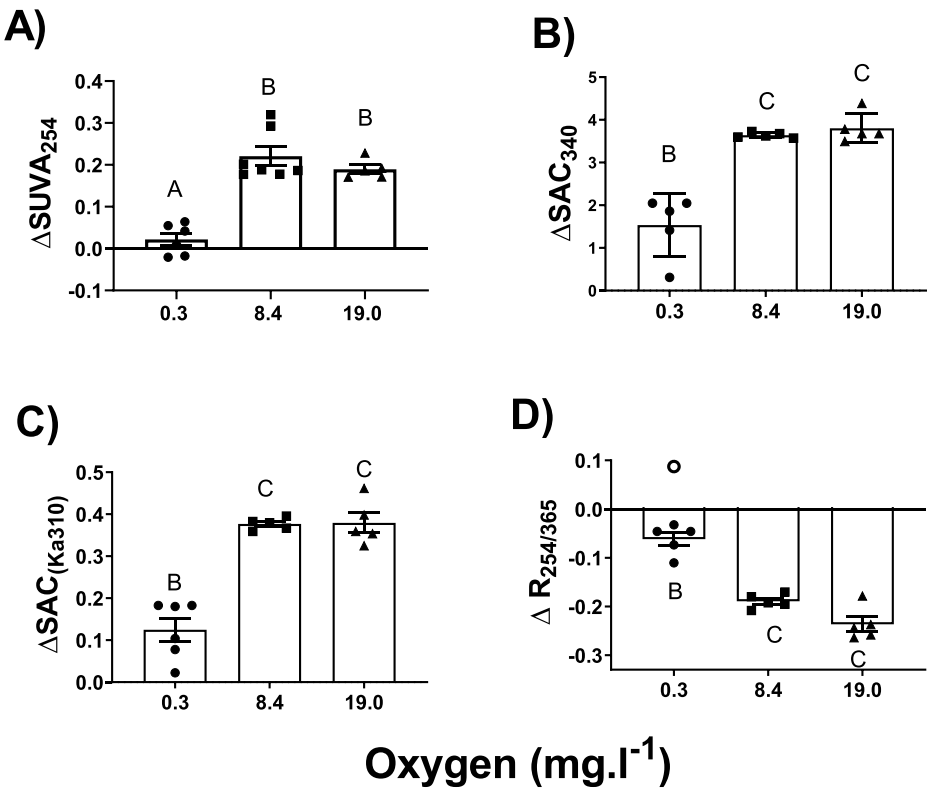

Fig. 2. Changes (Δ) in absorbance indices during photo-oxidation at three oxygen concentrations (near-anoxia, normoxia, hyperoxia) under reduced-UVR. (A) $\Delta SUVA_{254}$, (B) ΔSAC_{340}, C) ΔSAC_{Ka310}, and (D) $\Delta R_{254/365}$. See Fig. 1 legend for more details. Kruskal-Wallis Analysis of Variance followed by Dunn's multiple comparisons tests was employed for $\Delta SUVA_{254}$ (Kruskal-Wallis$_{(3,16)}$ = 11.88, p = 0.0004). For all other indices, F-values were >27 and all p<0.0001. n = 5 to 6. Outliers removed from statistical consideration are plotted as 'o'. 'A' indicates no significant difference from dark controls.

Table 4
Comparison of the ratios of mean absorbance or fluorescence loss under near-anoxia and normoxia (Δnear-anoxia/Δnormoxia): n ranged from 4 to 6. The treatments were photo-oxidized under either complete or reduced-UVR. Nearly all radiation <350 nm had been removed in the reduced-UVR treatment. There were no significant absorbance losses in the reduced-UVR/near-anoxia treatment at wavelengths <290 nm and >340 nm, eliminating comparisons denoted by a —.Note that ratios <1 indicate that losses were smaller in the reduced-UVR treatment than in the complete-UVR treatment.

Index	Ratio (Δnear-anoxia/Δnormoxia)		Difference
	Complete-UVR (2018)	Reduced-UVR (2015)	in Ratios
$SUVA_{254}$	0.61	—	—
SAC_{340}	0.70	0.30	0.40
SAC_{Ka310}	0.73	0.34	0.39
$R_{254/365}$	0.35	—	—
$Slope_{275–295}$	0.59	—	—
$Slope_{350–400}$	(nsd)	—-	
HA 370 nm	0.92 (nsd)**	0.74	0.18
HA 325 nm	1.13 (nsd)**	0.63	0.50
HA 300 nm	0.84 (nsd)**	0.58	0.26
HA 250 nm	na	0.48	–

** Δnear-anoxia and Δnormoxia were not significantly different
na = not available.

3.2. Slope indices

Changes in the slope indices differed between the complete-UVR and the reduced-UVR exposures. Note that all initial slopes were negative, thus as a slope becomes more negative, the Δslope is positive and vice versa. Under complete-UVR exposure, the steepness of $Slope_{275–295}$ increased (became more negative) in all treatments, but more so with oxygen present (Fig. 5A). $Slope_{350–400}$ became more positive (flatter) with no significant differences among oxygen treatments (Fig. 5B). Under reduced-UVR, $Slope_{275–295}$ and $Slope_{350–400}$ were not calculated in the near-anoxia treatment because absorbance had not changed significantly throughout the slope region. Under oxic conditions, $Slope_{275–295}$ became steeper and $Slope_{350–400}$ did not change: normoxic and hyperoxic slopes were not significantly different (Figs. 5C and D).

3.3. Fluorescence

Redox state can affect the intensity of fluorescence and the location of maximum fluorescence (Cory and McKnight, 2005). Dark control fluorescence intensities and maxima did not change across oxygen treatments, except for an increase in fluorescence in 2018 at 370 nm (data not shown). Nor were there significant differences in the location of maximum fluorescence between the dark control and light treatments with three exceptions: 2015, 370 nm excitation, hyperoxia; 2018, 300 nm excitation, hyperoxia; and 2018, 300 nm excitation, normoxia. The lack of noticeable shifts in the other profiles may be due to the 10-nm spacing of emission data

Two fluorescence indices were monitored during the experiments: FA and HA. Under complete-UVR, ΔFA fluorescence saw gains (negative) or no change, except for a loss (positive) at near-anoxia, 300 nm excitation (Figs. 6B and C). Under reduced-UVR, ΔFA fluorescences were equal and positive (losses) across oxygen concentrations (Figs. 7B-D).

Under both UVR treatments (Figs. 6A-C, Fig. 7A-D), losses (positive) in ΔHA fluorescence were larger as oxygen concentration increased. Under complete-UVR the increase was gradual. Under reduced-UVR, the loss in HA fluorescence was significantly smaller under near-anoxia than under normoxia or hyperoxia (Table 4, Figs. 6A and C, 7A-D). The ratios of Δnear-anoxia/Δnormoxia showed no significant diferences under complete-UVR and 26% to 52% losses under reduced-UVR (Table 4).

4. Discussion

4.1. Interaction of oxygen and light

In near lack of oxygen, photo-oxidation is depressed, and when coupled with a loss of the shorter UV wavelengths, it nearly collapses

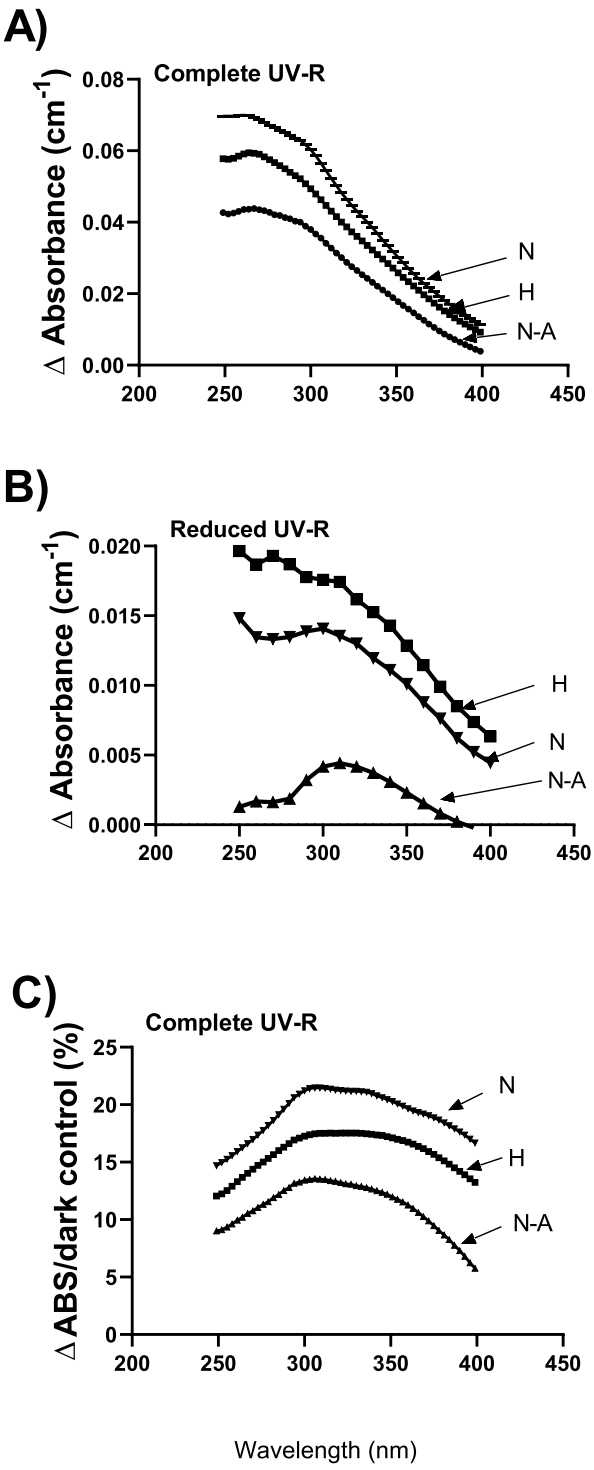

Fig. 3. Δabsorbance profiles for Rio Negro DOC exposed to hyperoxic (curve H), normoxic (curve N) or near-anoxic (curve N-A) conditions under either (A) complete-UVR or (B) reduced-UVR (wavelengths >350 nm). Δabsorbance was calculated by subtracting the average of the light absorbance data from the corresponding average dark absorbance for each measured wavelength from 249 to 400 nm. (C) proportion of absorbance lost during photo-oxidation (Δabsorbance/dark control absorbance) under complete-UVR.

(Fig. 4). Examining the changes in absorbance patterns and indices highlights how oxygen and light interact and where each is most needed for photo-oxidation.

The quality of the results depends on the efficacy of the dark controls which account for all non-light driven changes in absorbance. Bacteria

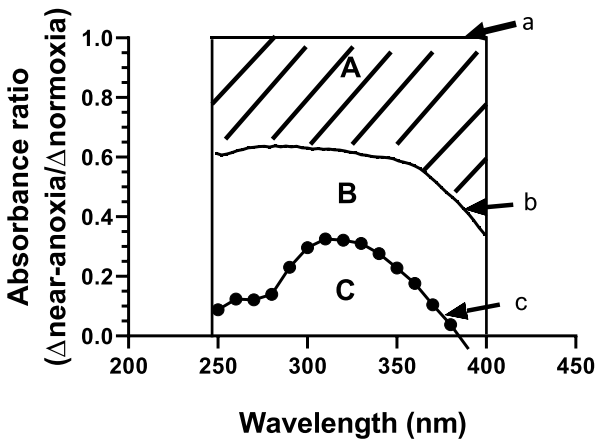

Fig. 4. Profiles of Δnear-anoxia/Δnormoxia absorbance ratios for DOC exposed to complete-UVR (curve b) or reduced-UVR (wavelengths >350 nm) (curve c). These curves were calculated from the data in Figs. 3A and B. The profiles are bounded by a rectangle between 0 and 1 on the y-axis and 249 to 400 nm on the x-axis. The flat line labelled 'a' at Y = 1.0 is hypothetical and represents a line of no impact of near-anoxia on absorbance loss. The top area 'A' is the proportionate loss in photo-oxidation due to lack of oxygen across wavelengths from 249 to 400 nm. The area 'B+C' is the proportion of photo-oxidation that remains under complete-UVR but lack of oxygen. And 'C' is the proportion of photo-oxidation that remains across wavelengths under reduced-UVR and lack of oxygen.

are the principal concern. If bacterial populations change at different rates in the light and dark, estimates of photo-oxidative absorbance loss will be affected. We considered possible scenarios and concluded that the dark controls were unlikely to be compromised by changes in bacterial populations (Supplementary Table S1).

During photo-oxidation, radiant energy degrades DOC both directly by breaking molecular bonds, and indirectly by exciting electrons which can (1) form ROS by interacting with oxygen, (2) dissipate energy as heat or fluorescence, or (3) move to other electron orbits and interactions (Cooper and Klymkowsky, 2019; McKay 2020).

The most important result of the study was observed in the reduced-UVR experiment: the Δabsorbance profile under normoxic conditions extended back to the shortest wavelengths measured (250 nm), even though radiation below 300 nm had been removed and only limited radiation occurred between 300 and 350 nm (Fig. 3B, curve N). Under these conditions, the highest levels of absorbance loss still occurred at ≤ 320 nm, similar to the pattern under complete-UVR (Figs. 3A and B, curves N). Del Vecchio and Blough (2004) made similar observations when they irradiated DOC in a glycerol solution, with a specific wavelength: 266, 318, 355, 390, 460 and 535 nm. They monitored the loss in absorbance over time from 250 to 550 nm. Absorbance was lost first at the initiating wavelength and then radiated out. At irradiance wavelengths ≥ 355 nm, the loss of absorbance became broader and extended out beyond 250 nm. The patterns were characterized by a slight dip around 254 nm and a consistent peak at 300 nm, as seen in our data (Fig. 3A & B curves N). The spreading out of absorbance loss is a characteristic of DOC photo-oxidation.

In reduced-UVR/near-anoxia, photo-oxidation processes broke down (Fig. 3B curve N-A). Significant loss of absorbance occurred only between 290 and 340 nm (Fig. 3B curve N-A). This indicates that the extensive loss of absorbance at shorter wavelengths under reduced-UVR/normoxia was due to processes involving oxygen. Two possible secondary reactions could explain these patterns: either the action of ROS or of excited electrons on bonds associated with shorter wavelength absorbance which incorporated oxygen on degradation.

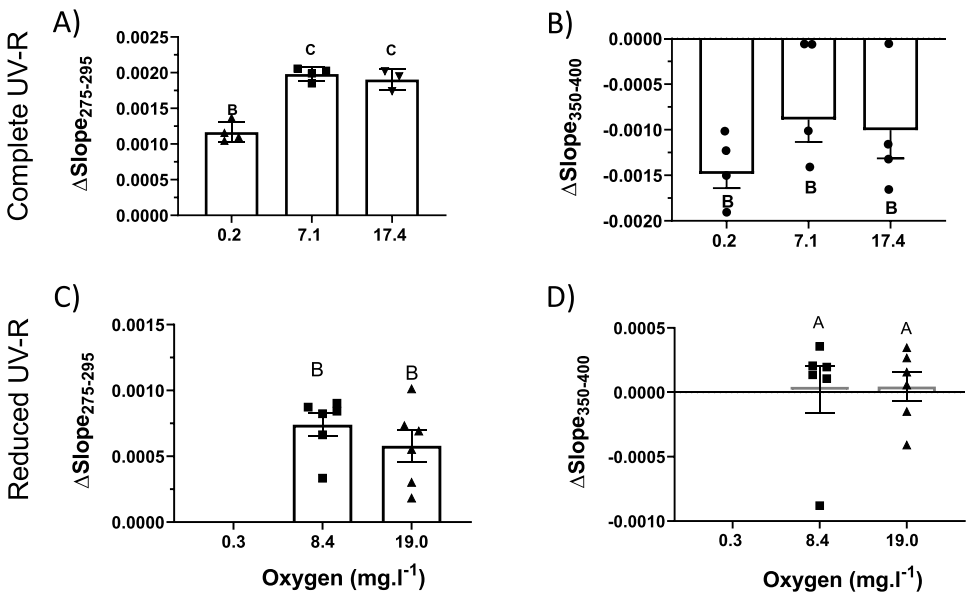

Fig. 5. Changes in absorbance slope metrics after photo-oxidation at three oxygen concentrations (near-anoxia, normoxia, hyperoxia) under two UVR treatments. Complete-UVR: (A) $\Delta Slope_{275\text{-}295}$, and (B) $\Delta Slope_{350\text{-}400}$, n = 4, 4 and 3. Reduced-UVR: C) $\Delta Slope_{275\text{-}295}$, and (D) $\Delta Slope_{350\text{-}400}$. n = 6, 6 and 6. Under near-anoxia/reduced-UVR absorbances did not change between the light and dark treatments at <290 and >340 nm. Therefore, no data were calculated for the anoxia treatment. See Fig. 1 legend for more details. Note all initial slopes were negative, thus as a slope becomes more negative the Δslope is positive and vice versa. (A) $\Delta Slope_{275\text{-}295}$, (Kruskal-Wallis$_{(3,11)}$ = 7.48, p <0.0068), (B) $\Delta Slope_{350\text{-}400}$,(Kruskal-Wallis$_{(3,11)}$ (nsd)) (C) $\Delta Slope_{275\text{-}295}$ (, (Kruskal-Wallis $_{(3,18)}$ n.s.d.), (D) $\Delta Slope_{350\text{-}400}$, (Kruskal-Wallis$_{(2,12)}$ n.s.d.). Different letters above the bars indicate significant differences.

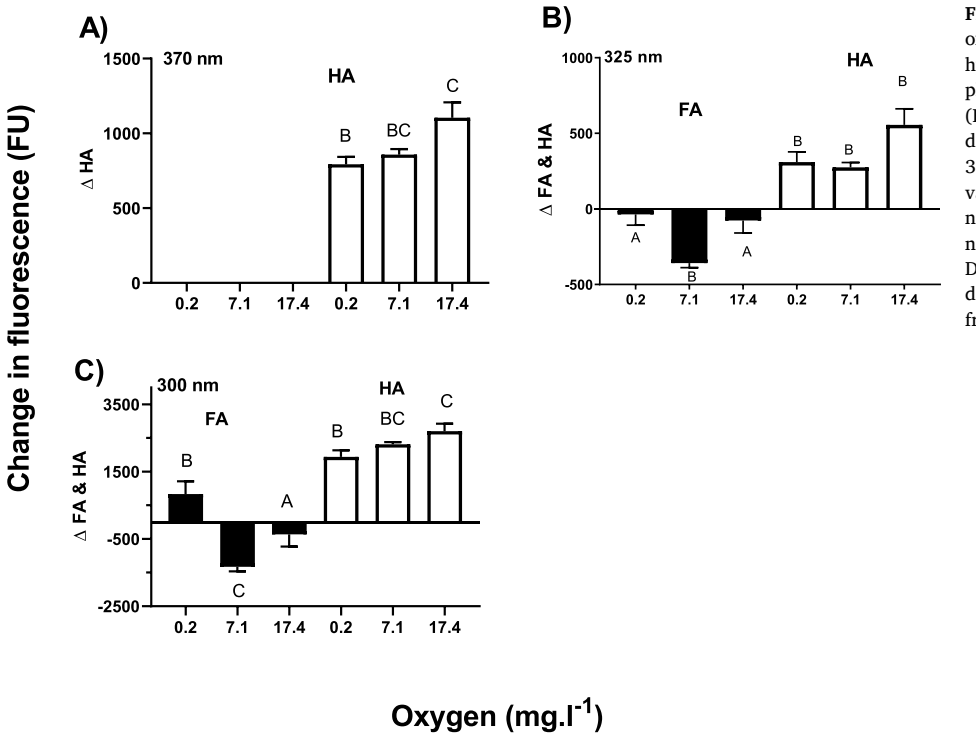

Fig. 6. Changes (Δ) in fluorescence during photo-oxidation under near-anoxia, normoxia and hyperoxia under complete-UVR. Panels A, B and C plot the change in fluorescence of humic acid-like (HA), and fulvic acid-like (FA) moieties (as defined in Table 3) at excitation wavelengths 370, 325 and 300 nm respectively. All significant HA F-values were >5.1 and p-values < 0.038. FA at 300 nm: Kruskal-Wallis = 7.144, p = 0.0097: FA at 325 nm: $F_{(2,9)}$ = 7.156, p = 0.0138. n = 4, 4, 3. Different letters above the bars indicate significant differences. 'A' indicates no significant change from dark control.

4.2. DOC processing during photo-oxidation

We used $Slope_{275–295}$, $Slope_{350–400}$ and the $R_{254/365}$ to follow the responses in DOC processes during photo-oxidation; namely, the degradation of larger molecules into smaller molecules (Helms et al., 2008). We concluded that (1) both UVB radiation and secondary processes involving oxygen contributed to processing DOC from larger to smaller molecules along the 275 - 295 nm absorbance region, ($Slope_{275–295}$) (Fig. 5A and C); (2) breaking down larger aromatic molecules, which absorb in the 350 - 400 nm range, is dependent on radiant energy alone. Oxygen is not involved in changes to $Slope_{350–400}$ (Fig. 5B and D); (3) oxygen is involved in their further breakdown as seen by the much higher absorbance losses under normoxia than under near-anoxia (Fig. 4, curves b and c); and (4) the relatively small change in $R_{254/365}$ in near-anoxia compared with normoxia suggests that the rate of production of smaller molecules is oxygen dependent and reduced compared with their conversion to CO_2 under near-anoxia (Table 4).

In the reduced-UVR/anoxia treatment, Δabsorbances in the 340–400 nm region were smaller than expected considering that UVA radiation in the bottles was estimated at ~56% of sub-surface levels (Methods 2.1), and UVA breakdowns DOC (Dahlén et al., 1996; Senga et al., 2018). The lack of change in $Slope_{350–400}$ under normoxia and hyperoxia (reduced-UVR/near-anoxia) reflect the small Δabsorbances (Fig. 5D). UVA intensity was insufficient to cause slope changes.

Johannsson et al., (2020) examined the depth profile of DOC absorbance changes due to photo-oxidation in their study of the Rio

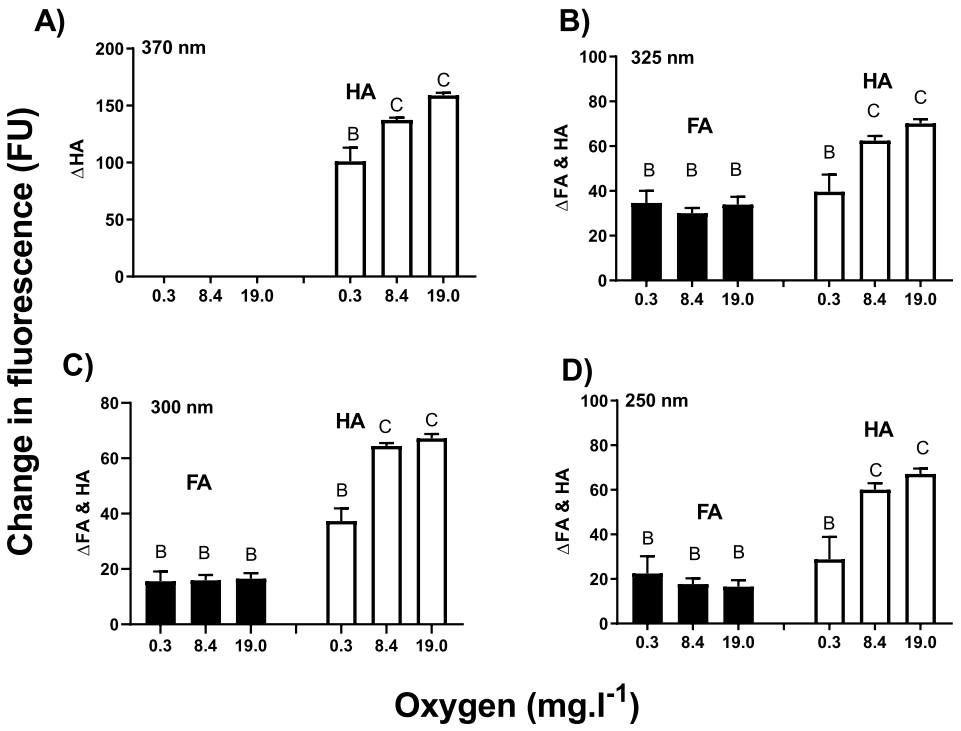

Fig. 7. Changes (Δ) in fluorescence during photo-oxidation under near-anoxia, normoxia and hyperoxia under reduced-UVR. Panels A, B, C and D plot the change in fluorescence of humic acid-like (HA), and fulvic acid-like (FA) moieties (defined in Table 3) at excitation wavelengths 370, 325, 300 and 250 nm respectively. All HA F-values were >11 and p-values < 0.0010. n = 5 to 6. FA p-values were >0.05. Different letters above the bars indicate significant differences.

Negro. They used the same experimental procedures as employed in the present study, running their experiment in quartz tubes suspended in a pool of Rio Negro water. By re-analyzing their data set, we were able to examine the changes in $\Delta Slope_{275–295}$ and $\Delta Slope_{350–400}$ within the top 8 cm of the water column. If $Slope_{350–400}$ is determined by shorter UVR, which penetrates only a few centimeters into the water column, then we should see significant changes in $\Delta Slope_{350–400}$ in the upper few centimeters but not deeper in the water column. On the other hand, if photo-oxidation is maintained by oxidative processes when shorter wavelengths no longer penetrate into the water column, $\Delta Slope_{275–295}$ should decrease with depth but still change significantly at greater depths than $\Delta Slope_{350–400}$. That is what occurred – $Slope_{350–400}$ changed only in the upper few centimeters and was not significantly different from zero as of 5 cm depth (Fig. 8). Approximately 5% of UVB and 25% of UVA would reach 5 cm depth in the pool, based on Beer-Lambert calculations of absorbance loss by wavelength in unfiltered Rio Negro pool water. $Slope_{275–295}$ changed throughout the depth examined (Fig. 8).

The importance of changes (or lack of changes) in $Slope_{350–400}$ are not easy to interpret. Absorbance slopes characterize the absorbance properties of the underlying DOC structure. Flattening of $Slope_{350–400}$ is associated with shifts in mean molecular weight towards smaller molecules – a breakdown of larger molecules (Helms et al., 2008). Our data show that $Slope_{350–400}$ is changed by UVR, but not oxygen (Fig. 5B), and that in the absence of change in $Slope_{350–400}$, absorbance losses continue in the presence of oxygen (Fig. 3B curves H & N). So how to reconcile a lack of change in slope with continued loss of absorbance.

Change in $R_{254/365}$ is a measure of the process of photo-oxidation: $R_{254/365}$ follows the relative increase in the abundance of smaller molecules as the larger DOC molecules are broken down. $\Delta R_{254/365}$ is

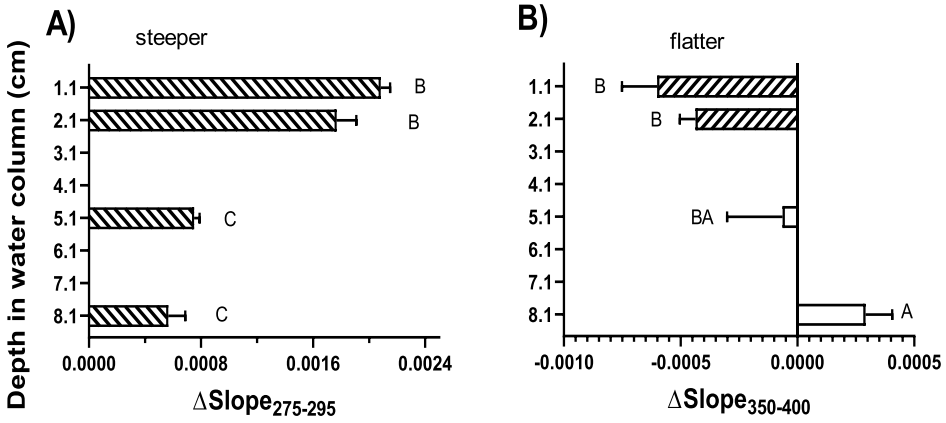

Fig. 8. Photo-oxidative induced changes in absorbance slope metrics with depth in the water column. (A) $_{Slope275-295}$, (B) $Slope_{350-400}$. Note: Δpositive slopes become steeper, and Δnegative slopes become flatter. The slopes were calculated from absorbance data published by Johannsson et al. (2020). Different letters beside the bars indicate significant differences. 'A' indicates no significant change from the dark controls. Those bars also have no pattern.

governed by the relative rates of two photo-oxidative processes - the loss of small molecules through production of CO_2, and the replenishment of small molecules through the degradation of larger molecules. Under complete-UVR, the majority of absorbance indices and production of CO_2 were reduced by 30% – 40% between the normoxic and near-anoxia treatments (Table 4, Patel-Sorrentino et al., 2004; Johannsson, Ferreira, Wood and Val, unpublished data). $\Delta R_{254/365}$, however, was reduced by 65%. The relatively small change in $R_{254/365}$ under near-anoxia reflects a change in photo-oxidative processes. $SUVA_{254}$, the numerator of $R_{254/365}$, was depressed by 39%; not enough to explain the 65% drop in $R_{254/365}$. The absorbance loss at longer wavelengths under near-anoxia was less than that of the shorter wavelengths (Fig. 4, curve b), indicating that a lack of oxygen reduced the rate of breakdown of larger molecules. The imbalance between the losses and gains of small molecules would explain the small $\Delta R_{254/365}$. This conclusion is supported by Helms et al., (2008), who observed a 70% smaller increase in% smaller molecules and a decreased conversion rate from high to low molecular weight compounds under low oxygen conditions (21% air saturation).

The above considerations provide insights into how areal (m^{-2}) photo-oxidation is affected by changing oxygen and UVR conditions with depth. Under normoxic conditions at depths beyond the penetration of significant amounts of UVB (280–320 nm) radiation, gradients in UVA and PAR, and then just PAR, maintain photo-oxidation. Helms et al., (2008) showed that increases in $Slope_{275–295}$ and decreases in $Slope_{350–400}$ tracked conversion of larger to smaller molecules. At depth, when $Slope_{350–400}$ ceases changing between 5 and 8 cm depth, larger molecules in this region are no longer being cleaved into smaller molecules. ROS and/or excited electrons from PAR maintain the breakdown of molecules across the absorbance spectrum. Changes in absorbance indices were observed down to 14 cm depth (Johannsson et al., 2020). Without PAR radiation, the production of CO_2 and smaller molecules would quickly be curtailed in the water column. Under significantly reduced oxygen conditions, near or at anoxia, photo-oxidation would be reduced by approximately a third at the water's surface in the Rio Negro (Patel-Sorrentino et al., 2004; Table 4), and would collapse with depth as the transmittance of shorter wavelengths is diminished and ROS and oxygen are not available to maintain the processes of photo-oxidation.

4.3. Fluorescence, photo-oxidation in oxygen and light gradients

FA and HA fluorophores are affected by different portions of the radiation spectrum in conjunction with oxygen. Losses of HA fluorescence occurred in all treatments, indicating that longer wavelengths are involved (Figs. 6A and C, Figs. 7A, B, C and D). Johannsson et al., (2020) showed that HA fluorescence was lost to greater depths than changes in absorbance. This supports the participation of PAR, in losses of HA fluorescence. The significant difference between normoxia and near-anoxia under reduced-UVR, but not complete-UVR, suggests that UVB may also play some role and that oxygen increases the losses.

UVB together with oxygen drives gains in FA fluorophores (Fig. 6B and C). FA fluorescence losses occurred in situations where UVB was absent (Figs. 7B, C and D) or oxygen was not present to work in conjunction with UVB (Fig. 7B, and C near-anoxia). Senga et al., (2018) and Dahlén et al., (1996) observed losses of FA fluorescence and concentration when only UVA was applied during photo-oxidation, supporting the importance of specifically UVB in production of FA fluorophores. The loss of FA fluorescence does not require oxygen or UVB radiation.

Changes in fluorescence are not always indicators of changes in the abundance of fluorophores because their excitation can lead to a change in redox state as well as alteration of the molecule (Cory and McKnight, 2005). In three instances, the position of peak fluorescence shifted during photo-oxidation toward shorter wavelengths, indicative of a more oxidized state. In each instance, the shift would not affect the results of the experiments. This suggests that changes in fluorescence were generally changes in concentration of fluorophores.

5. Conclusions

- Oxygen and radiation type (UVB, UVA and PAR) interact to control different aspects of photo-oxidation of DOC.
- Oxygen coupled with UVA and PAR radiation are essential to produce ROS at depth in the water column. The ROS maintains photo-oxidation across all absorbance wavelengths where penetration of shorter UVR wavelengths decreases. Without oxygen, the processing of larger molecules would be depressed in the 275–295 nm region ($Slopes_{275–295}$) and the return of CO_2 to the atmosphere would be reduced at all depths. Detailed relationships between oxygen and photo-oxidation across oxygen concentrations from anoxia to normoxia are not known and need to be determined.
- The upper surface waters, where UVB radiation is high, support higher rates of conversion of larger to smaller molecules through the 275–295 nm and 350–400 nm absorbance regions. In addition, FA-like fluorophores were created only in the presence of UVB and oxygen.
- The present day decreases in oxygen in many aquatic environments are likely affecting photo-oxidation processes and may impact the global carbon cycle.

Declaration of Competing Interest

The authors declare that they have no known competing financial interests or personal relationships that could have appeared to influence the work reported in this paper.

Acknowledgements

Special thanks to the personnel at INPA - Maria de Nazaré Paula da Silva for her overall assistance, Rogério Santos Pereira for technical troubleshooting, and Reginaldo Oliveira and Thiago Nacimento for general help. Also, many thanks to the constructive and encouraging comments of two anonymous reviewers.

Funding

Work in Brazil was supported by FAPEAM (062.01187/2017), CNPq (465540/2014–7) and CAPES (Financial Code 001) through the INCT-ADAPTA grant to ALV, and a Ciência sem Fronteiras grant to ALV and CMW, and in Canada by the Natural Sciences and Engineering Research Council of Canada (NSERC) Discovery grants to CMW (RGPIN-2017–03843, RGPIN/473–2012) and DSS (RGPIN-2015–04414). MSF was the recipient of a Post-Doctoral fellowship from the Brazilian centre for Improvement of Higher Education Personnel (Coordenação de Aperfeiçoamento de Pessoal de Nível Superior, CAPES). ALV received a Research Fellowships from CNPq (303930/2014–4; 306716/2019–4).

The funding sources played no role in the research presented here.

Supplementary materials

Supplementary material associated with this article can be found, in the online version, at doi:10.1016/j.watres.2021.117332.

References

Al-Reasi, H.A., Smith, D.S., Wood, C.M., 2012. Evaluating the ameliorative effect of natural dissolved organic matter (DOM) quality on copper toxicity to *Daphnia magna*: improving the BLM. Ecotoxicology 21, 525–537.

Al-Reasi, H.A., Wood, C.M., Smith, D.S., 2013. Characterization of freshwater natural dissolved organic matter (DOM): mechanistic explanations for protective effects against metal toxicity and direct effects on organisms. Environ. Int. 59, 201–207.

Abbt-Braun, G., Lankes, U., Frimmel, F.H., 2004. Structural characterization of aquatic humic substances - the need for a multiple method approach. Aquat. Sci. 66, 151–170.

Amaral, J.H.F., Farjalla, V.F., Melack, J.M., Kasper, D., Scofield, V., Barbosa, P.M., Forsberg, B.R., 2019. Seasonal and spatial variability of CO_2 in aquatic environments of the central lowland Amazon basin. Biogeochemistry 143, 133–149.
Amon, R.M.W., Brenner, R., 1996. Photochemical and microbial consumption of dissolved organic carbon and dissolved oxygen in the Amazon River system. Geochim. Cosmochim. Acta 60, 1783–1792.
Carder, K.L., Steward, R.G., Harvey, G.R., Ortner, P.B., 1989. Marine humic and fulvic acids: their effects on remote sensing of ocean chlorophyll. Limnol. Oceanogr. 34, 68–81.
Chowdhury, S., 2013. Trihalomethanes in drinking water: effect of natural organic matter distribution. Water SA 39, 1–7.
Published by Cooper, M., Klymkowsky, M., 2019. CLUE: appendix Spectroscopy. In: Klymkowsky, Michael, Cooper, Melanie (Eds.), Creative Commons Attribution-Noncommercial-Sharealike 4.0 International License.
Cory, R.M., McKnight, D.M., 2005. Fluorescence spectroscopy reveals ubiquitous presence of oxidized and reduced quinones in dissolved organic matter. Environ. Sci. Technol. 39, 8142–8149.
Cory, R.M., McNeill, K., Cotner, J.P., Amado, A., Purcell, J.M., 2010. Singlet oxygen in the coupled photochemical and biochemical oxidation of dissolved organic matter. Environ. Sci. Technol. 44, 3683–3689.
Cory, R.M., Ward, C.P., Crump, B.C., Kling, G.W., 2014. Sunlight controls water column processing of carbon in arctic fresh waters. Science 345, 925–928.
Curtis, P.J., Schindler, D.W., 1997. Hydrologic control of dissolved organic matter in low-order Precambian Shield lakes. Biogeochemistry 36, 125–138.
Dahlén, J., Bertilsson, S., Petterson, C., 1996. Effects of UV-A irradiation on dissolved organic matter in humic surface waters. Environ. Int. 22, 501–506.
Daniel, M.H.B., Montebelo, A.A., Bernardes, M., Omette, J.P., de Camargo, P.B., Krusche, A.V., Ballester, M.V.R., Victoria, R., Martinelli, L.A., 2002. Effects of urban sewage on dissolved oxygen, dissolved inorganic and organic carbon, and electrical conductivity of small streams along a gradient of urbanization in the Piracicaba River Basin. Water Air Soil Pollut. 136, 189–206.
Del Vecchio, R., Blough, N.V., 2004. On the origin of the optical properties of humic substances. Environ. Sci. Technol. 38, 3885–3891.
Dias, D.A., Ghiggino, K.P., Smith, T.A., Scollary, G.R., 2010. Wine bottle colour and oxidative spoilage. Final Report to Grape and Wine Research and Development Corporation. School of Health and Biomedical Sciences. RMIT University, Melbourne, Australia.
Diaz, R.J., Breitburg, D.L., 2009. The hypoxic environment. In: Fish Physiology, 27. Academic Press, pp. 1–23.
Gao, H., Zepp, R., 1998. Factors influencing photoreactions of dissolved organic matter in a coastal river of the southeastern United States. Environ. Sci. Technol. 32, 2940–2946.
Gonsior, M., Peake, B.M., Cooper, W.T., Podgorski, D., D'Andrilli, J., Cooper, W.J., 2009. Photochemically induced changes in dissolved organic matter identified by ultrahigh resolution fourier transfor ion cycloton resononance mass spectrometry. Environ. Sci. Technol. 43, 698–703.
Granéli, W., Lindell, M., de Faria, B.M., Esteves, F., 1998. Photo-production of dissolved inorganic carbon in temperate and tropical lakes – dependence on wavelength band and dissolved organic carbon concentration. Biogeochemistry 43, 175–195.
Granéli, W., Lindell, M., Tranvik, L., 1996. Photo-oxidative production of dissolved inorganic carbon in lakes of different humic content. Limnol. Oceanogr. 96, 698–706.
Hansen, A.M., Kraus, T.E.C., Pellerin, B.A., Fleck, J.A., Downing, B.D., Bergamaschi, B.A., 2016. Optical properties of dissolved organic matter (DOM): effects of biological and photolytic degradation. Limnol. Oceanogr. 61, 1015–1032.
Hayase, K., Tsubota, H., 1985. Sedimentary humic-acid and fulvic-acid as fluorescent organic materials. Geochim. Cosmochim. Acta 49, 159–163.
Helms, J.R., Stubbins, A., Ritchie, J.D., Minor, E.C., Kieber, D.J., Mopper, K., 2008. Absorption spectral slopes and slope ratios as indicators of molecular weight, source, and photobleaching of chromophoric dissolved organic matter. Limnol. Oceanogr. 53, 955–965.
Johannsson, O.E., Smith, D.S., Sadauskas-Henrique, H., Cameron, G., Wood, C.M., Val, A. L., 2017. Photo-oxidation processes, properties of DOC, reactive oxygen species (ROS), and their potential impacts on native biota and carbon cycling in the Rio Negro (Amazonia, Brazil). Hydrobiologia 789, 7–29.
Johannsson, O.E., Ferreira, M.S., Smith, D.S., Crémazy, A., Wood, C.M., Val, A.L., 2020. Effects of natural light and depth on rates of photo-oxidation of dissolved organic carbon in a major black-water river, the Rio Negro, Brazil. Sci. Total Environ. 733, 139193.
Kirk, J.T.O, 1994. Light and Photosynthesis in Aquatic Ecosystems, 2nd ed. Cambridge University Press, New York.
Lindell, M.J., Rai, H., 1994. Photochemical oxygen consumption in humic waters. Archiv für Hydrobiologie. Beihefte. Ergebnisse der Limnologie 43, 145–155.
Lou, T, Xie, H, 2006. Photochemical alteration of the molecular weight of dissolved organic matter. Chemosphere 65, 2333–2342.
Lou, T., Xie, H., Chen, G., Gagné, J-P., 2006. Effects of photodegradation of dissolved organic matter on the binding of beno(α)pyrene. Chemosphere 64, 1204–1211.
McKay, G., 2020. Emerging investigator series: critical review of photophysical models for the optical and photochemical properties of dissolved organic matter. Environ. Sci.: Processes Impacts 22, 1139–1165.
Patel-Sorrentino, N., Mounier, S., Luca, Y., Benaim, J.Y., 2004. Effects of UV- visible irradiation on natural organic matter from the Amazon basin. Sci. Total Environ. 321, 231–239.
Rasera, M.F.I., Krusche, A.V., Richey, J.E., Ballester, M.V.R., Victória, R.I., 2013. Spatial and temporal variability of pCO_2 and CO_2 efflux in seven Amazonian Rivers. Biogeochemistry 116, 241–259.
Richey, J.E., Hedges, J.I., Devol, A.H., Quay, P.Q., 1990. Biogeochemistry of carbon in the Amazon River. Limnol. Oceanogr. 35, 352–371.
Scully, N.M., McQueen, D.J., Lean, D.R.S., Cooper, W.J., 1996. Hydrogen peroxide formation: the interaction of ultraviolet radiation and dissolved organic carbon in lake waters along a 43–75 N gradient. Limnol. Oceanogr. 41, 540–548.
Senga, Y., Naruoka, C., Moriai, S., Nohara, S., 2018. Characterizing the transformation of aquatic humic substances exposed to ultraviolet radiation using excitation-emission matrix fluorescence spectroscopy and PARAFAC. Inland Waters 8, 505–511.
Smith, V.H., Joye, S.B., Howard, R.W., 2006. Eutrophication in marine and freshwaters. Limnol. Oceanogr. 51, 351–355.
Spencer, R.G.M., Butler, K.D., Aiken, G.R., 2012. Dissolved organic carbon and chromophoric dissolved organic matter properties of rivers in the USA. J. Geophys. Res. 117, GO3001.
Vähätalo, A.V., Salonen, K, Salkinoja-Salonen, M, Hatakka, Annele, 1999. Photochemical mineralization of synthetic lignin in lake water indicates enhanced turnover of aromatic organic matter under solar radiation. Biodegradation 10, 415–420.
Val, A.L., Almeida-Val, V.M.F., et al., 1995. Fishes of the Amazon and their Environment: Physiological and Biochemical Aspects. In: Bradshaw, S.D., Burggren, W., Heller, H. C., Ishii, S., Langer, H., Neuweiler, G., et al. (Eds.), Zoophysiology Vol 32. Springer-Verlag, Berlin, p. 224.
Wang, X., Lou, T., Xie, H., 2009. Photochemical production of dissolved inorganic carbon from Suwannee river humic acid. Chin. J. Oceanogr. Limnol. 27, 570–573.
Ward, C.P., Cory, R.M., 2016. Complete and partial photo-oxidation of dissolved organic matter draining permafrost soils. Environ. Sci. Technol. 50, 3545–3553.
Weishaar, J.L., Aiken, G.R., Bergamaschi, B.A., Fram, M.S., Fugii, R, Mopper, K., 2003. Evaluation of specific ultraviolet absorbance as an indicator of the chemical composition and reactivity of dissolved organic carbon. Environ. Sci. Technol. 37, 4702–4708.
Wood, C.M., Al-Reasi, H.A., Smith, D.S., 2011. The two faces of DOC. Aquatic. Toxicol. 105S, 3–8.
Wu, R.S., 2002. Hypoxia: from molecular responses to ecosystem responses. Mar. Pollut. Bull. 45, 35–45.
Xie, H., Zafiriou, O.C., Cai, W-J, Zepp, R.G., Wang, Y., 2004. Photooxidation and its effects on carboxyl content of dissolved organic matter in two coastal rivers in the southeastern United States. Environ. Sci. Technol. 38, 4113–4119.
Zhang, Y., Xie, H., 2015. Photomineralization and photomethanification of dissolved organic matter in the Saguenay River surface water. Biogeochemistry 12, 6823–6836.
Technical Glass Products. 2020. Fused quartz/fused silica average transmittance curves. http://www.technicalglass.com/fused_quartz_transmission.html. Accessed latest March 23, 2020.